LA-UR -93-478

LA-UR--93-478

DE93 008706

Los Alamos National Laboratory is operated by the University of California for the United States Department of Energy under contract W-7405-ENG-36

TITLE START BROADENED PROFILES WITH SELF-CONSISTENT RADIATION TRANSFER AND ATOMIC KINETICS IN PLASMAS PRODUCED BY HIGH INTENSITY LASERS

AUTHOR(S) G. L. Olson
J. C. Comly
J. K. La Gattuta
D. P. Kilcrease

SUBMITTED TO Journal and Proceedings: Proceedings will be published as one issue of that Journal.

DISCLAIMER

Los Alamos National Laboratory
Los Alamos, New Mexico 87545

Stark Broadened Profiles with Self-Consistent Radiation Transfer and Atomic Kinetics in Plasmas Produced by High Intensity Lasers

Gordon L. Olson, Jack C. Comly, J. Kenneth La Gattuta, David P. Kilcrease
Los Alamos National Laboratory
Los Alamos, NM 87545

5th International Workshop on Radiative Properties of Hot Dense Matter
2 - 6 November 1992, Santa Barbara, CA

to appear in a special issue of:
Journal for Quantitative Spectroscopy and Radiative Transfer

STARK BROADENED PROFILES WITH SELF-CONSISTENT RADIATION TRANSFER AND ATOMIC KINETICS IN PLASMAS PRODUCED BY HIGH INTENSITY LASERS

GORDON L. OLSON, JACK C. COMLY, J. KENNETH LA GATTUTA, DAVID P. KILCREASE
Los Alamos National Laboratory, Los Alamos, NM 87545, U. S. A.

Abstract–Spectral line shapes and line strengths have long been used to diagnose plasma temperatures and densities. In dense plasmas, the additional broadening due to Stark effects give additional information about the plasma density. We present calculations that are self-consistent in that the radiation fields of the line transitions and the atomic kinetics are iterated to convergence. Examples are given for simple plasmas with temperature gradients, density gradients, and velocity fields. Then a more complex example of a laser produced plasma is presented.

1. INTRODUCTION

The proceedings of the previous conference in this series[1] contains excellent presentations dealing with the importance of spectroscopy in understanding plasmas. Parallel to advances in experimental spectroscopy, numerical techniques for the solution of the radiation transfer equation have improved significantly over the last few years[2-5]. Combined with recent improvements in personal computers and scientific workstations, it is now easily affordable to do steady-state one-dimensional radiative transfer coupled to atomic kinetics. The need for escape probabilities and other approximations should diminish in the future.

While experiments can be carefully designed to have uniform densities and temperatures,[6] they are the exception rather than the rule. Most experiments have density and temperature gradients and velocity fields. Many times, they are also strongly time dependent. This paper will deal with dense plasmas which have all of these complications. In the following section, the methods we use in calculating line profiles in dense plasmas are presented. Then in Sec. 3, line profiles are shown which arise in simple, but non-uniform plasmas. Section 4 discusses the radiation-hydrodynamics code used in the present calculations. Section 5 shows a laser-

plasma interaction calculation that comes from modeling an actual high intensity laser experiment.

2. STARK PROFILE-CODE MODIFICATIONS

Since the general formulation and assumptions used in calculating density-broadened line profiles are well documented,[7] and the specific approximations used in the profiles presented here are published,[8] we will concentrate on the changes we have made rather than the over-all theory.

Lee[8] made a significant contribution to line theory applications by using the APEX theory[9,10] and several well chosen approximations. The resulting code for calculating line shapes is dramatically faster than those previously available and makes line shape calculations practical on a personal computer. On a supercomputer, one can now do complex radiation-hydrodynamic simulations that include Stark-broadened line profiles.

In October of 1991, we obtained the then current version of Lee's line shape code. Although it had been optimized by using fast approximations for complicated physics, we found several places where we rewrote details so that calculations would vectorize on a Cray YMP. The largest single algorithmic change was to throw out the Doppler convolution routines which were based on fast Fourier transform (FFT) techniques. Because the frequency grid on which the profile is calculated is not uniform, it was necessary to interpolate the profile on to an equally-spaced grid, do the FFT, and then interpolate back on to the variable grid. We found that directly evaluating the convolution as a double integral on the original grid was four to five times faster than the FFT plus interpolation.

In the line code there are various integrals over probability distributions. If one is interested only in frequencies near line center, it is necessary only to do these integrals out to 15 normalized energy units. However, to reliably calculate far into the wings, we had to increased these integrals out to 35 units.

The largest physics change we made was to include the two temperature APEX theory presented by Kilcrease[11] elsewhere in this conference. In simulations of intense lasers, the ion and electron temperatures are often significantly different from each other. Adding the ability to have two temperatures vastly broadens the applicability of a line profile code.

Working with Magee[12] we made various changes that made the profile code more robust at higher densities. Magee also extended the tables of atomic

parameters down to hydrogen. Now the calculations can be done for hydrogen through iron.

Rather than show isolated, idealized profile shapes which can be found in other references, Figs. 1 and 2 show self-consistent calculations of the radiation emitted from a 10 micron thick slab of aluminum at a temperature of 600 eV with five different ion densities. These calculations are self-consistent in the that radiation field is solved iteratively until converged with the atomic kinetics equations. More details about the code used for this calculation are given in Sec. 4. Note that at low densities the lines are narrow and have essentially Doppler shapes. With increasing density the traditional Stark shapes appear. At the highest density shown, the line wings are dominated by the continuum intensity. The line from the upper quantum levels (n = 4 and above) disappear as their optical depths become less than the neighboring continuum optical depth.

3. EFFECTS OF PHYSICAL GRADIENTS

In most laboratory or astrophysical plasmas, there are density gradients, temperature gradients, and velocity fields. Figure 3 shows four different emitted shapes for the Lyman β line of aluminum. All four are from a 10 micron-thick slab with a baseline ion number density of 3×10^{21} cm^{-3} and temperature of 600 eV. The uniform case, labeled U, has no gradients or velocities and is the basic line shape produced by Lee's code.[8] The curve labeled with a T has a linear temperature drop of 100 eV from one side of the slab to the other. The curve labeled with a N, has a linear ion density decreasing from 3×10^{21} to 2×10^{21} cm^{-3} from one edge to the other. The curve labeled with a V has a parabolic velocity distribution ranging from zero on one surface to 6×10^{7} cm/s on the other surface. Note that the density and temperature gradients produce nearly the same emission line shape.

Figure 4 shows Lyman α and some of its satellites for the same conditions as in Fig. 3. Here the density and temperatures produce results that are not as similar as they were for Lyman β. The velocity field allows photons to escape that would have been trapped by self-absorption; therefore, the peak emission of Lyman α is larger with a velocity field, as well as being displaced in frequency. The satellites are very thin; therefore, velocity effects just spread out their emission in frequency, causing the emission peaks to drop. By measuring the intensities and shapes of several lines, one can model and deduce the combined effects of temperature and density gradients.

In standard treatments of line radiation transfer,[13] one can usually assume a line profile is symmetric. Most astrophysical plasmas have low enough densities that Stark effects are negligible so this is a reasonable assumption. This symmetry property allows significant savings in computer time and programming effort, even with non-zero velocities. Unfortunately, Stark profiles are in general non-symmetric, so none of these savings are available.

4. ZAP

ZAP is the name of the code that has been used to calculate the examples presented here. Although the above examples are steady-state solutions, ZAP is a general-purpose radiation-hydrodynamics code. The primary uses of ZAP are to model detailed atomic processes in x-ray lasers[14] and to model plasmas for spectroscopic diagnostics.

ZAP solves the one-dimensional Lagrangian hydrodynamics equations for slab, cylindrical, or spherical geometry. The numerical method uses a half-step-full-step algorithm with a staggered spatial mesh and a even time discretization. Either one or two energy balance equations are solved for one or two temperatures (ion and electron). Thermal conduction can be included for just electrons or both electrons and ions.

The radiation transfer in ZAP uses deterministic one-dimensional slab geometry methods. The non-LTE line transfer uses approximate operator iteration[4,5] and the equivalent-two-level-atom technique to solve the transfer equation consistently with the atomic kinetics rate equations. The line transfer includes the velocity and non-symmetrical profile complications mentioned in the previous section. Laser energy is deposited using a simple ray tracing scheme.

Some of the atomic data is generated with a family of Los Alamos codes[15,16] based on Hartree-Fock wave functions. From these codes, we get energy levels, oscillator strengths, and electron impact excitation rates. To produce configuration- and Rydberg-averaged atomic levels we have written our own automated codes to produce the atomic data bases. We use scaled hydrogenic electron impact excitation and ionization rates.[17-21] Photoionization cross sections are Z-scaled fits for each configuration.[22] Autoionization and dielectronic recombination can be included by explicitly using a doubly excited level or by using a net rate coefficient. In order to model plasmas produced by high intensity lasers, it was necessary to add multi-photon ionization and multi-photon inverse bremsstrahlung.

The atomic model used in the aluminum calculations presented here contains 309 energy levels from the once ionized through the totally stripped atom. Configuration-averaged levels are used for principle quantum numbers of 1, 2, and 3. In the highly stripped ions, the n = 4 levels are also configuration-averaged. In the near neutral ions, the n = 4 levels are Rydberg-averaged. In all ions, the n = 5, 6, and 7 energy levels are Rydberg-averaged. In order to include the autoionization and dielectronic recombination processes, doubly-excited levels are added to the Be-, Li-, and He-like ions. This also causes some satellite lines to appear in calculated spectra.

5. HIGH INTENSITY LASER PRODUCED PLASMA

The Los Alamos Bright Source Lasers (LABS) are KrF and XeCl lasers.[23,24] Briefly, the LABS I system is KrF at 248 nm wavelength, with an energy of 30 mJ, a pulse width of 700 fs, and a peak intensity of 3×10^{17} W/cm^2. The same quantities for LABS II are 308 nm, 0.25 J, 300 fs, and 10^{19} W/cm^2. Time integrated spectroscopy of solid aluminum targets[25,26] shows strong emission lines from the hydrogen- and helium-like ion stages with line widths of 4 to 6 eV. With the lower intensity laser, the He-like lines dominate the spectrum. With LABS II, the H-like lines are stronger, comparable to the He-like line strengths.

A surprise in these spectra is that the lines from higher n levels are not significantly broader than those from lower n. If the emission occurs from a dense plasma, one would expect that the line widths would generally increase with increasing n. This surprise was a major motivation for adding Stark broadened profiles to the radiation transfer abilities in ZAP. Our goal was to simulate these plasmas in order to understand where the line emission originates.

These lasers have a moderate intensity (10^9 to 10^{12} W/cm^2) prepulse that illuminates the target for 1 to 10 ns before the main pulse arrives. This prepulse produces a plasma blowoff with which the mainpulse will then interact. According to ZAP simulations, the main pulse heats the plasma to between 1 and 5 keV, depending on assumptions about how much energy is absorbed and reflected at the laser's critical surface.

Figures 5 and 6 show time integrated theoretical spectra calculated with ZAP for typical laser parameters of LABS I and II, respectively. The lines in Fig. 6 are broader and have more of the typical Stark shapes than the lines in Fig. 5. This indicates that the higher intensity laser get more of its energy into higher densities.

Unfortunately, the experimental data do not show this behavior. The experimental line widths and shapes differ very little between LABS I and II spectra.

This discrepancy between theory and experiment suggests that something is wrong in our assumptions in modeling the laser plasma interaction. One possibility is that, at the higher intensities, plasma instabilities cause the laser photons to be absorbed at lower densities than the critical density. This suggestion and others will be explored in future research and publications.

6. CONCLUSIONS

In summary, we have discussed improvements to an existing package for calculating Stark broadened line profiles. We have presented simple example calculations and more complicated examples with density gradients, temperature gradients, and velocity fields. The ZAP code which has the capability to deal with all these complications has been outlined. Finally, a full radiation-hydrodynamic simulation has been presented for comparison to actual experiments.

In conclusion, it appears that all the practical tools are available for doing steady-state radiation transfer and atomic kinetics calculations on workstation computers. Full rad-hydro calculations still require mainframe computers. Our LABS I calculations typically take 50 CPU hours on a Cray YMP, and the LABS II calculations take more than 100 CPU hours.

REFERENCES

1. *Radiative Properties of Hot Dense Matter* (Edited by W. Goldstein, *et al.*) World Scientific (1991).
2. *Methods in Radiative Transfer* (Edited by W. Kalkofen) Cambridge University Press (1984).
3. *Numerical Radiative Transfer* ((Edited by W. Kalkofen) Cambridge University Press (1987).
4. G. L. Olson, L. H. Auer, and J. R. Buchler, *JQSRT* **35**, 431 (1986).
5. G. L. Olson and P. B. Kunasz, *JQSRT* **38**, 325 (1987).
6. P. T. Springer, *et al.*, *Phys. Rev. Let.* **69**, 3735 (1992).
7. H. R. Griem, *Spectral Line Broadening by Plasmas*, Academic Press, NY (1974).
8. R. W. Lee, *JQSRT* **40**, 561 (1988).
9. J. W. Dufty, D. B. Boercker, and C. A. Iglesias, *Phys. Rev.* **31A**, 1681 (1985).
10. C. A. Iglesias, H. DeWitt, J. Lebowitz, D. MacGowan, and W. Hubbard, *Phys. Rev.* **31A**, 1698 (1985).
11. D. P. Kilcrease, *JQSRT*, this proceedings.
12. N. H. Magee, private communication.
13. D. Mihalas, *Stellar Atmospheres, 2nd Ed.*, W. H. Freeman and Co., SF (1978).
14. G. L. Olson, J. K. La Gattuta, and J. C. Comly, *Int. Colloquium on X-ray Lasers*, Inst. Phys. Conf. Ser. No. 116, IOP Publishing Ltd, 329 (1991).
15. J. Abdallah, Jr., R. E. H. Clark, and R. D. Cowan, *Theoretical Atomic Physics Code Development I – CATS: Cowan Atomic Structure Code*, LA-11436-M, Vol. 1, Los Alamos National Laboratory, (1988).
16. R. E. H. Clark, *et al.*, *Theoretical Atomic Physics Code Development II – ACE: Another Collisional Excitation Code*, LA-11436-M, Vol. 2, Los Alamos National Laboratory, (1988).
17. L. B. Golden and D. H. Sampson, *J. Phys. B* **10**, 2229 (1977).
18. D. H. Sampson and L. B. Golden, *J. Phys. B* **11**, 541 (1978)
19. L. B. Golden, D. H. Sampson, and K. Omidvar, *J. Phys. B* **11**, 3235 (1978)
20. D. L. Moores, L. B. Golden, and D. H. Sampson, *J. Phys. B* **13**, 385 (1980)
21. L. B. Golden and D. H. Sampson, *J. Phys. B* **13**, 2645 (1980)
22. R. E. H. Clark, private communication.
23. J. P. Roberts, A. J. Taylor, P. H. Y. Lee, and R. B. Gibson, *Opt. Lett.* **13**, 734 (1988).
24. A. J. Taylor, *et al*, *Ultrafast Phenomena VII*, Springer Series in Chemical Physics, **53**, 104, Springer Verlage, Berlin (1991)
25. J. A. Cobble, G. T. Schappert, L. A. Jones, A. J. Taylor, G. A. Kyrala, and R. D. Fulton, *J. Appl. Phys.* **69**, 3369 (1991).
26. G. A. Kyrala, *et al*, *Appl. Phys. Lett.*, **60**, 2195 (1992).

FIGURE CAPTIONS

1. The radiation emitted by a 10 micron-thick slab of aluminum at 600 eV and five different ion densities shows the n = 1 to 2 transitions of the helium- and hydrogen-like ions.
2. Same as for Fig. 1, except this is for the higher energy transitions.
3. The Lyman β line of aluminum is shown for a uniform slab (U), one with a temperature gradient (T), one with a density gradient (N), and one with a velocity field (V). Details are given in the text.
4. The Lyman α line of aluminum and some of its satellites are shown for the cases of Fig. 3.
5. A theoretical time-integrated spectrum for LABS I conditions. Each resonance line is labeled. The weaker lines on the low energy sides of the strong lines are satellite lines.
6. The same as Fig. 5 for LABS II conditions.

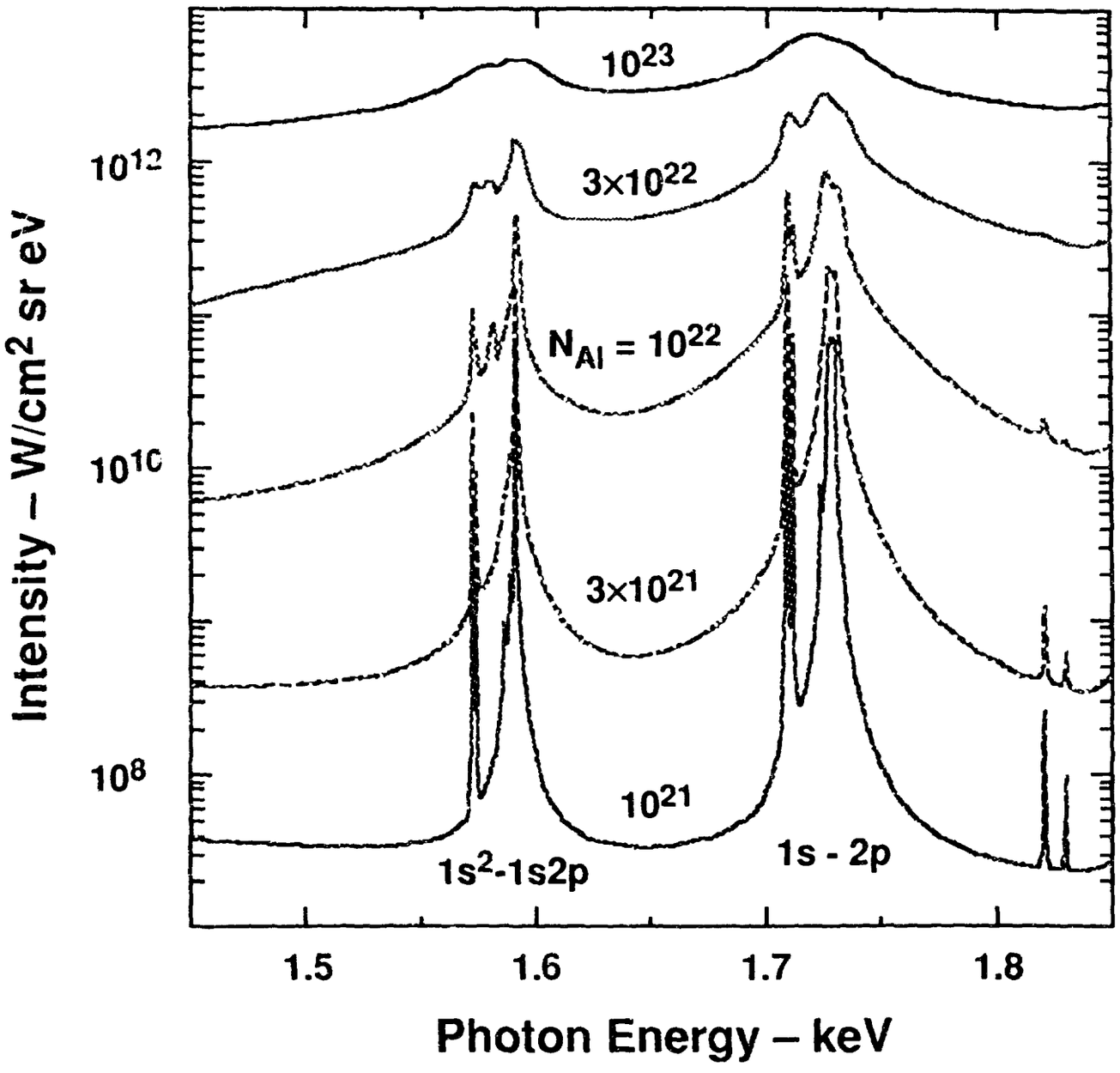
10^{23}
10^{12}
3×10^{22}
$N_{Al} = 10^{22}$
10^{10}
3×10^{21}
10^{8}
10^{21}
$1s^2$-1s2p
1s - 2p
1.5
1.6
1.7
1.8
Photon Energy – keV
Intensity – W/cm^2 sr eV

Fig 1

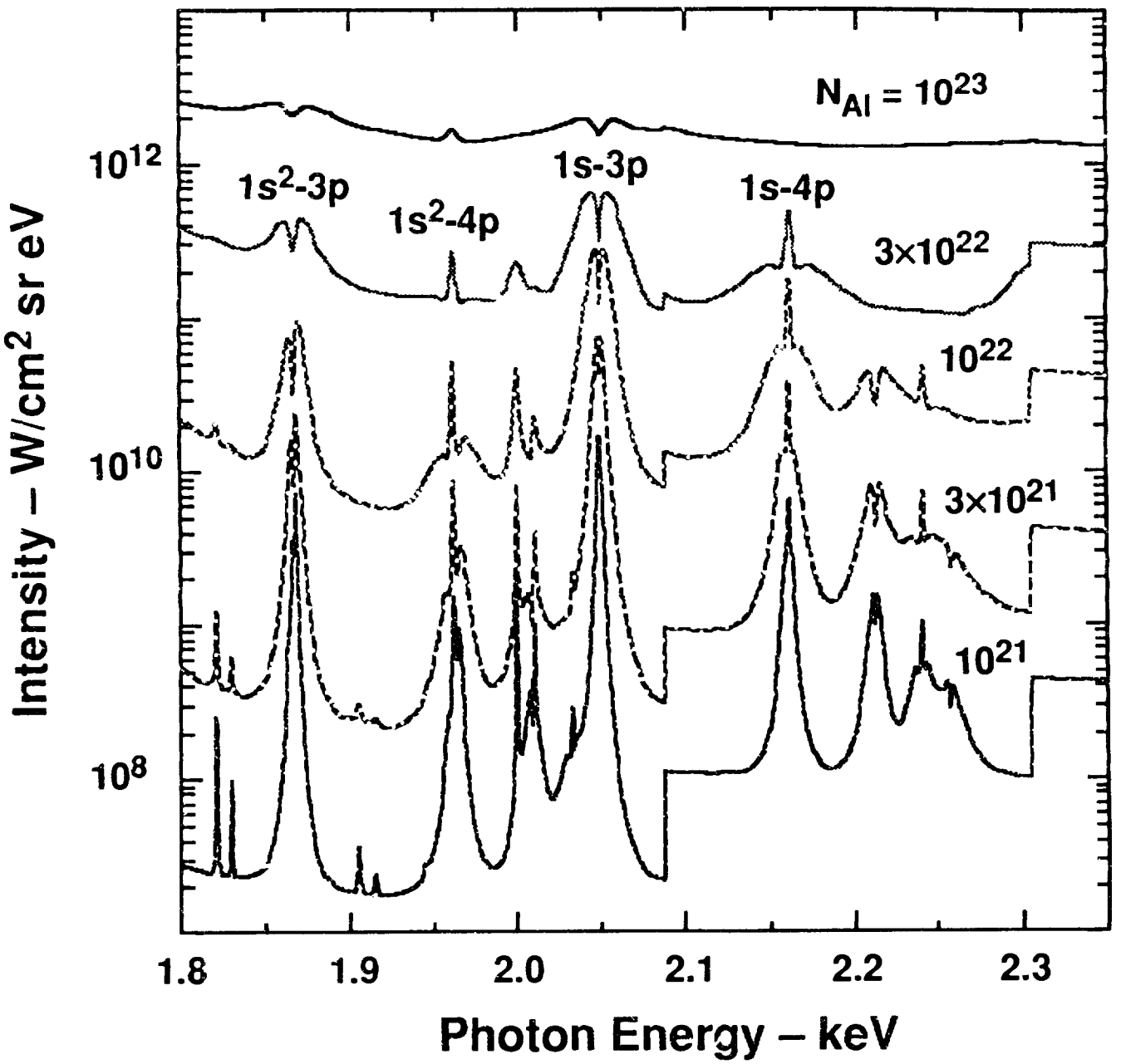
$N_{Al} = 10^{23}$
10^{12}
$1s^2$-3p
$1s^2$-4p
1s-3p
1s-4p
3×10^{22}
10^{22}
10^{10}
3×10^{21}
10^{21}
10^8
Intensity – W/cm^2 sr eV
1.8
1.9
2.0
2.1
2.2
2.3
Photon Energy – keV

Fig. 2

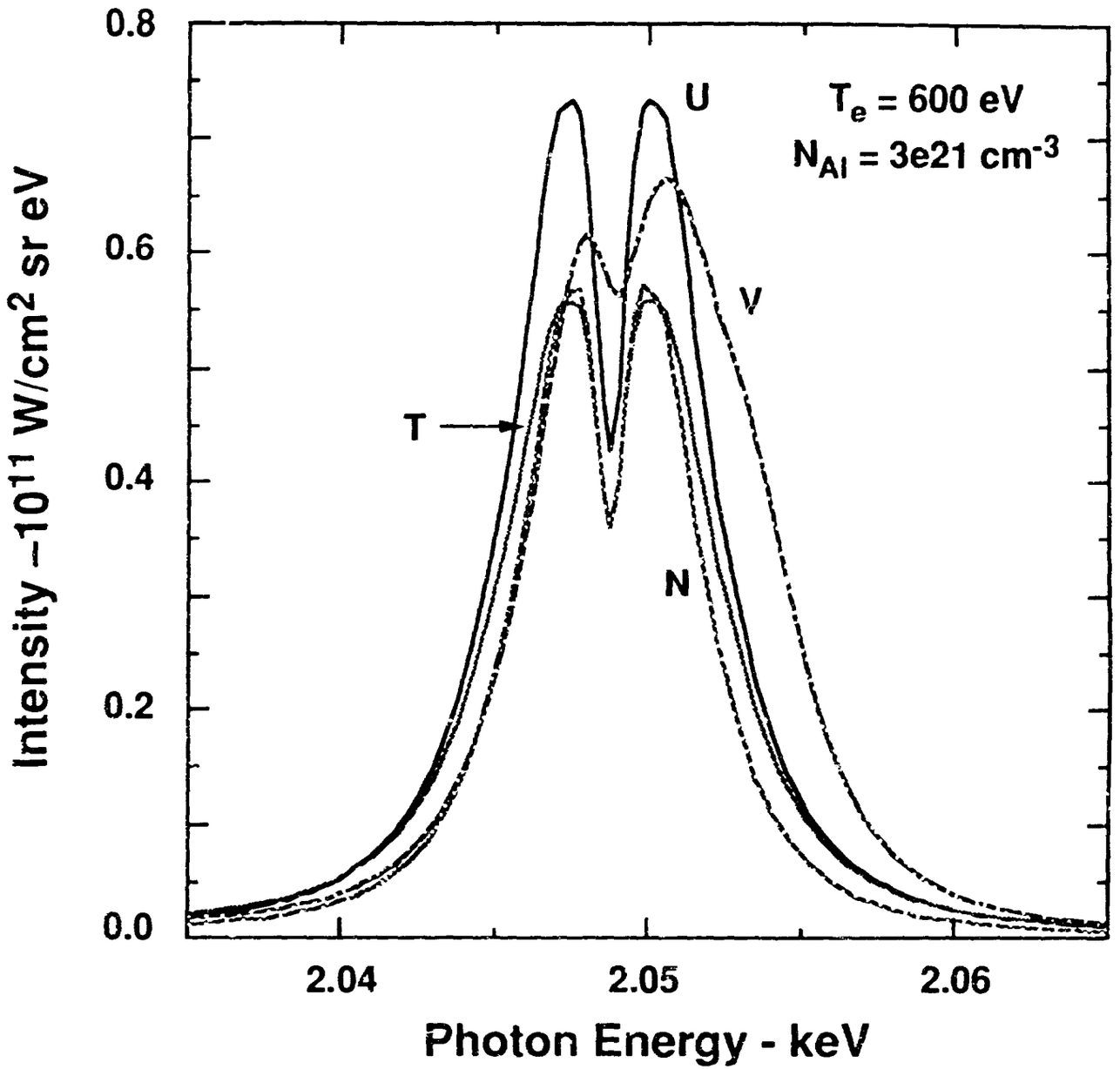
0.8
0.6
0.4
0.2
0.0
Intensity –10^11 W/cm^2 sr eV
2.04
2.05
2.06
Photon Energy - keV
U
V
T
N
T_e = 600 eV
N_Al = 3e21 cm^-3

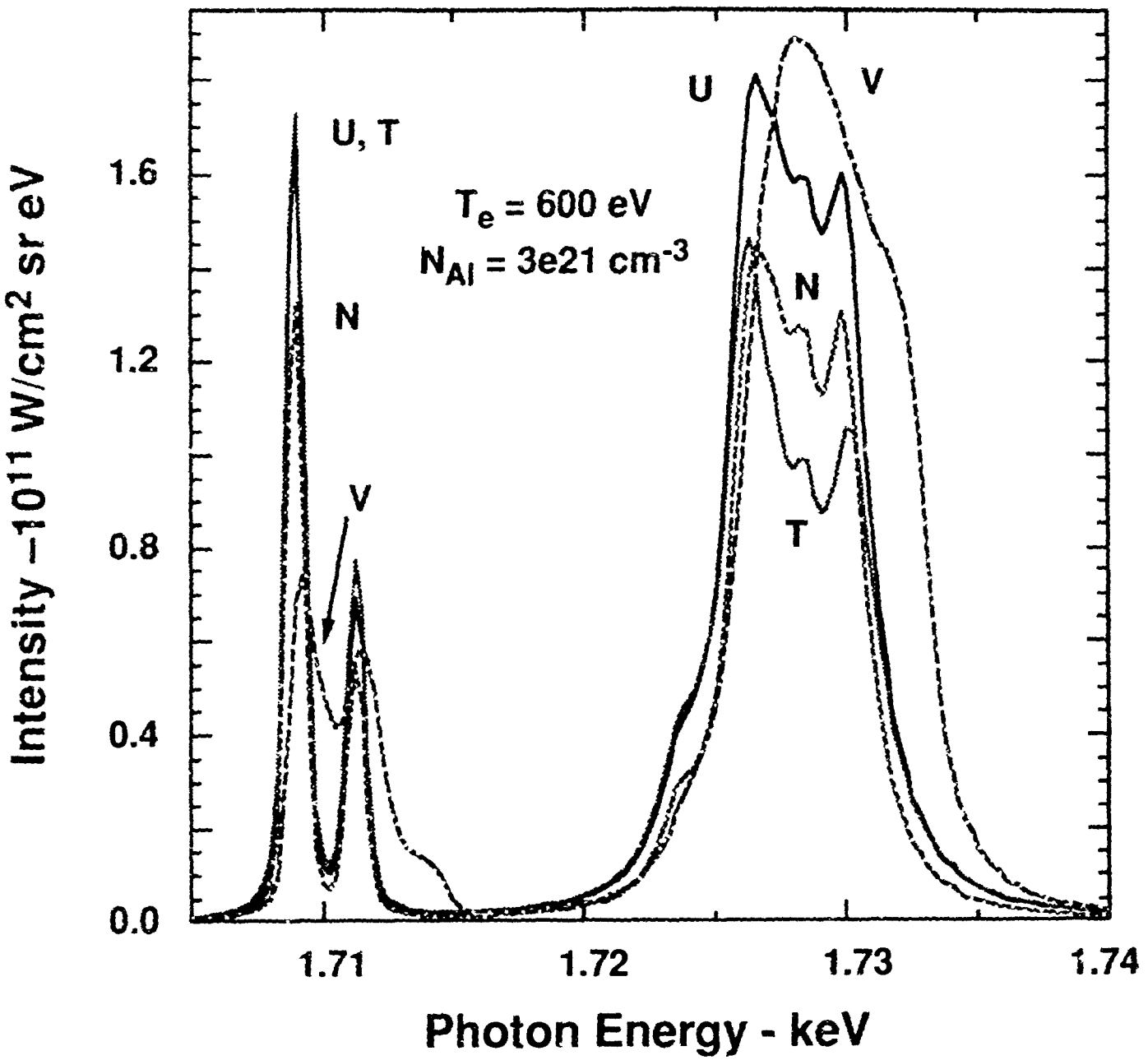
U, T
N
V
U
V
N
T
T_e = 600 eV
N_{Al} = 3e21 cm^{-3}
Intensity -10^{11} W/cm^2 sr eV
0.0
0.4
0.8
1.2
1.6
1.71
1.72
1.73
1.74
Photon Energy - keV

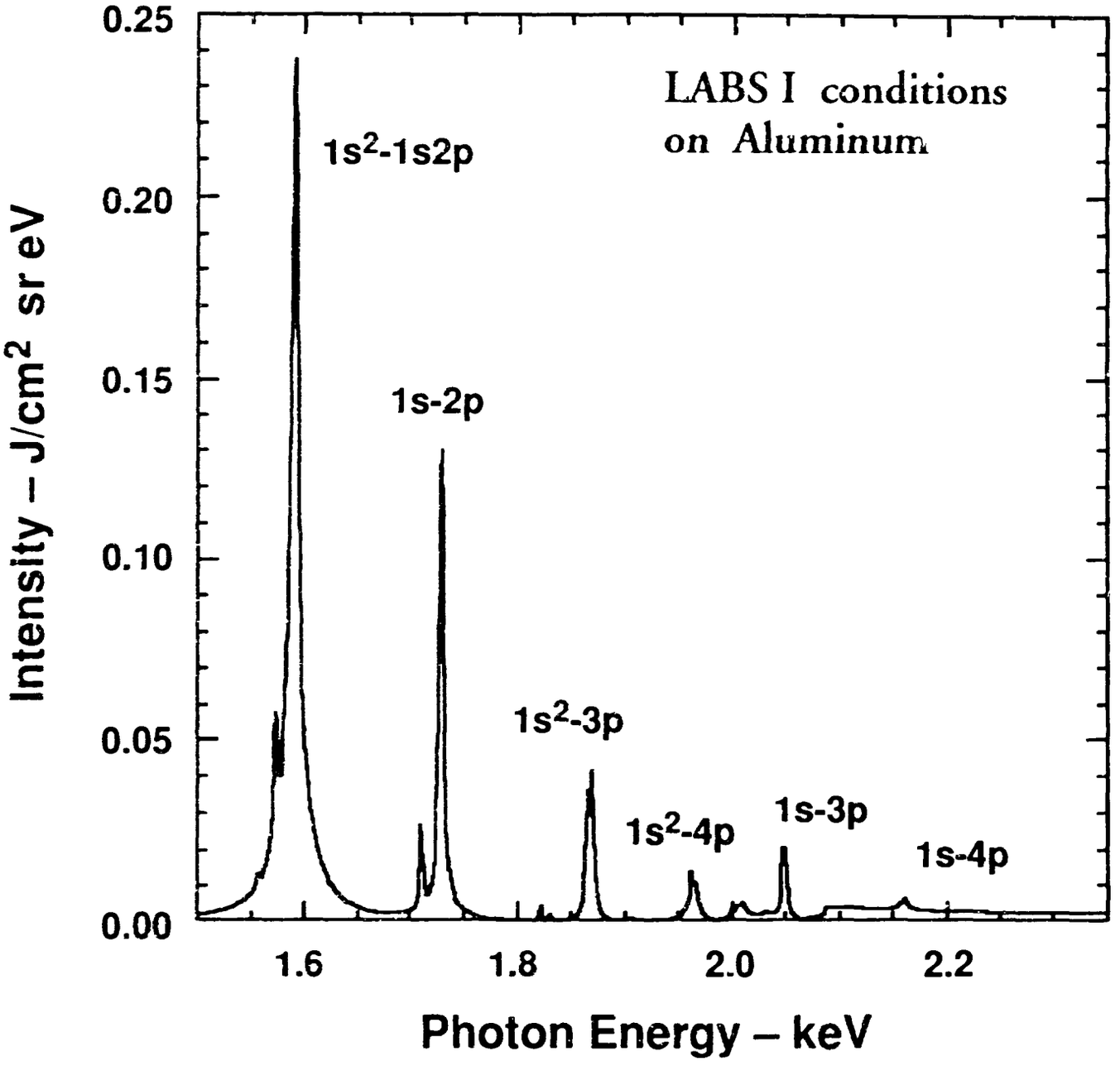
LABS I conditions
on Aluminum
1s²-1s2p
1s-2p
1s²-3p
1s²-4p
1s-3p
1s-4p
0.25
0.20
0.15
0.10
0.05
0.00
1.6
1.8
2.0
2.2
Intensity – J/cm² sr eV
Photon Energy – keV

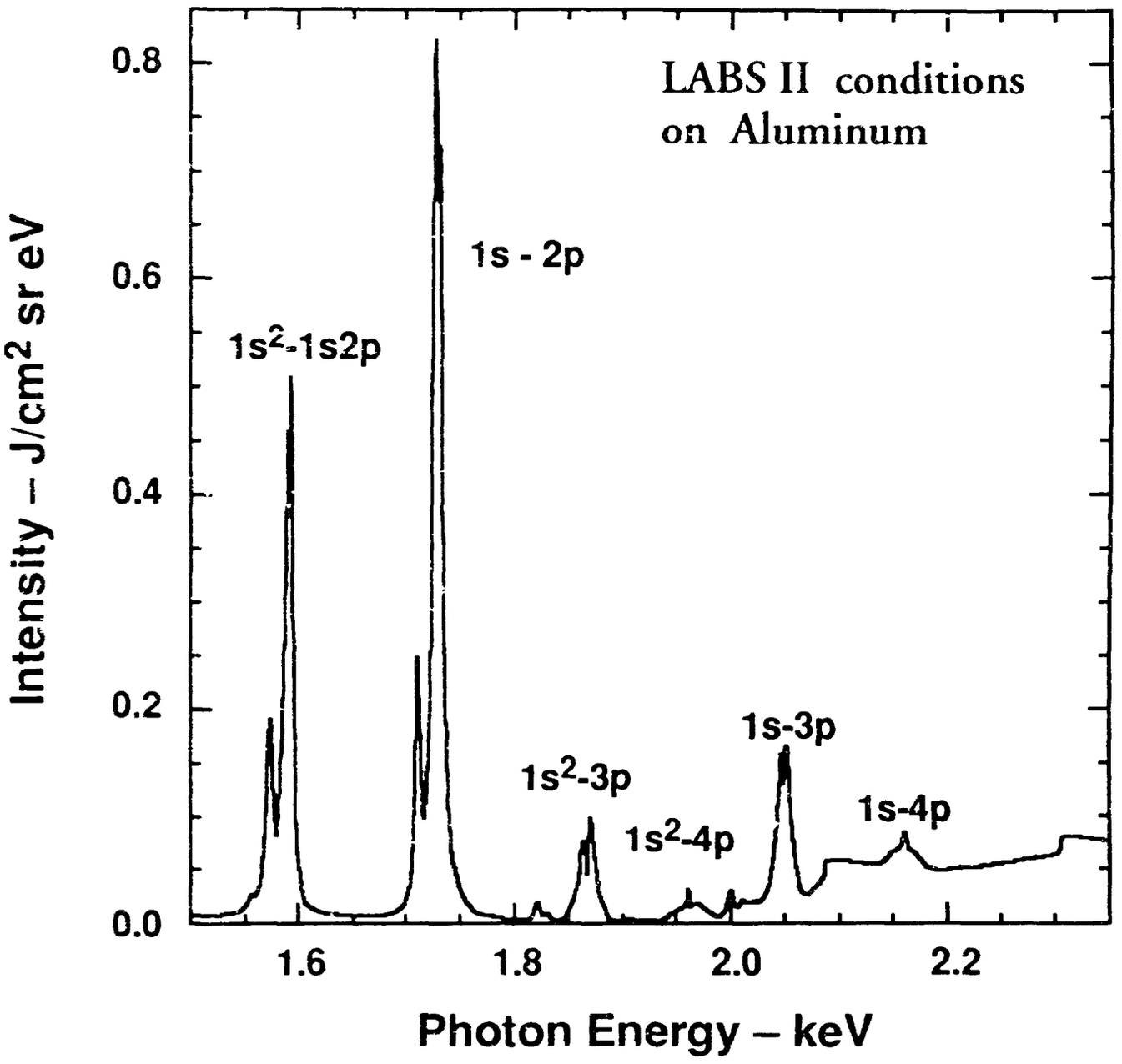
LABS II conditions
on Aluminum
1s - 2p
1s²-1s2p
1s²-3p
1s²-4p
1s-3p
1s-4p
Intensity – J/cm² sr eV
Photon Energy – keV
0.0
0.2
0.4
0.6
0.8
1.6
1.8
2.0
2.2